

AN ENERGETIC BLAST WAVE FROM THE DECEMBER 27 GIANT FLARE OF THE SOFT γ -RAY REPEATER 1806-20

X. Y. WANG¹, X. F. WU¹, Y. Z. FAN^{2,3}, Z. G. DAI¹ AND B. ZHANG²

¹Department of Astronomy, Nanjing University, Nanjing 210093, China; xywang@nju.edu.cn,
xfwu@nju.edu.cn, dzg@nju.edu.cn

² Department of Physics, University of Nevada, Las Vegas, NV 89154, USA, yzfan@physics.unlv.edu,
bzhang@physics.unlv.edu

³ Purple Mountain Observatory, Chinese Academy of Sciences, Nanjing 210008, China

Draft version October 23, 2018

ABSTRACT

Recent follow-up observations of the December 27 giant flare of SGR 1806-20 have detected a multiple-frequency radio afterglow from 240 MHz to 8.46 GHz, extending in time from a week to about a month after the flare. The angular size of the source was also measured for the first time. Here we show that this radio afterglow gives the first piece of clear evidence that an energetic blast wave sweeps up its surrounding medium and produces a synchrotron afterglow, the same mechanism as established for gamma-ray burst afterglows. The optical afterglow is expected to be intrinsically as bright as $m_R \simeq 13$ at $t \lesssim 0.1$ days after the flare, but very heavy extinction makes the detection difficult because of the low galactic latitude of the source. Rapid infrared follow-up observations to giant flares are therefore crucial for the low-latitude SGRs, while for high-latitude SGRs (e.g. SGR 0526-66), rapid follow-ups should result in identification of their possible optical afterglows. Rapid multi-wavelength follow-ups will also provide more detailed information of the early evolution of a fireball as well as its composition.

Subject headings: gamma rays: bursts—ISM: jets and outflows— stars: individual (SGR 1806-20)

1. INTRODUCTION

Soft γ -ray repeaters (SGRs) distinguish themselves from classical gamma-ray bursts (GRBs) by their repetitive, soft bursts coming from nearby sources, likely strongly magnetized neutron stars dubbed “magnetars” (Thompson & Duncan 1995). Giant flares are rare events from SGRs, each characterized by an initial hard spike with more than a million Eddington luminosity and a pulsating tail persisting for hundreds of seconds (Mazets et al. 1979; Hurley et al. 1999; Borkowski et al. 2004). A giant flare was recorded on 2004 December 27 from SGR 1806-20 (Borkowski et al. 2004; Hurley et al. 2004; Mazets et al. 2004; Palmer et al. 2004; Smith et al. 2005). In comparison with previous ones, this flare is exceptionally strong with an isotropic energy of gamma-ray emission larger than 8×10^{45} ergs (Boggs et al. 2005), given a source distance $d = 15.1$ kpc (Corbel & Eikenberry 2004).

Afterglow emission from giant flares was first detected from SGR 1900+14 at radio frequencies (Frail et al. 1999). The radio afterglow of the December 27 giant flare from SGR 1806-20 was detected about 7 days after the flare with a flux density at 8.46 GHz approximately 100 times brighter than the peak flux density of the SGR 1900+14 radio afterglow (Gaensler et al. 2005; Cameron et al. 2005). Generally, the multi-frequency radio afterglow light curves display a power law decay behavior with time during the observational time from one week to one month after the flare, which is quite similar to the afterglows of cosmological GRBs. But the decay rate at higher frequencies (e.g. 8.46 GHz) is larger than that at lower frequencies (e.g. 240 MHz) and the spectra clearly show a gradual steepening with time (Cameron et al. 2005).

Cheng & Wang (2003) suggested the possibility that the radio afterglow of the SGR 1900+14 giant flare might

be explained with the same mechanism as established for GRB afterglows (Mészáros & Rees 1997), i.e. the emission from the expanding blast wave that forms when the outflow from the SGR interacts with the surrounding interstellar medium (ISM). However, the data of that radio afterglow are too sparse for us to make a firm conclusion. The radio afterglow of the December 27 flare has much more abundant data of the light curves which was detected from 240 MHz to 8.46 GHz in frequency and from a week to a month after the flare in time. The angular size of the source was also measured for the first time. In this *Letter*, we will show that this radio afterglow gives the first piece of clear evidence that an energetic blast wave sweeps up its surrounding medium and produces a synchrotron afterglow.

2. THE BLAST WAVE MODEL FOR THE RADIO AFTERGLOW

It was suggested by Huang et al. (1998) that relativistic fireballs similar to those in classic GRBs may exist in SGR bursts. Thompson & Duncan (2001) proposed that the extraordinarily high peak luminosity $L > 10^6 L_{\text{Edd}}$ (where L_{Edd} is the Eddington luminosity), hard spectrum and rapid variability of the initial spike emission of giant flares imply that the spike emission must originate from a relativistically expanding fireball with the initial Lorentz factor of at least several in order to avoid the pair production problem. Such a relativistic outflow, after emitting the hard spike, should retain some energy and then drives a blast wave expanding into the surrounding medium.

2.1. *The angular size and constraint on the flare energy*

Now let’s first consider the dynamics of a blast wave that is driven by the relativistic outflow and expands into the ISM. The blast wave will be gradually deceler-

ated by the swept-up ISM and enter the non-relativistic phase at $t_{\text{nr}} = (3E/4\pi nm_p c^5)^{1/3} = 4.5E_{46}^{1/3} n_0^{-1/3}$ d, where E is the isotropic kinetic energy of the blast wave, c is the speed of light, n is the number density of ISM, m_p is the proton mass, and we have used the usual notation $a \equiv 10^n a_n$ in c.g.s. units except that the observer's time t is in unit of day. So, for $E_{46}/n_0 < 4$, the blast wave must have entered the non-relativistic phase during the observational time frame ($t > 7$ d). During this non-relativistic phase, the speed (in units of c) and the radius of the blast wave are given by $\beta = [12E/(125\pi nm_p c^5 t^3)]^{1/3} = 0.4E_{46}^{1/5} t_1^{-3/5} n_0^{-1/5}$ and $R = 5\beta ct/2 = 2.6 \times 10^{16} E_{46}^{1/5} t_1^{2/5} n_0^{-1/5}$ cm respectively (Cheng & Wang 2003). The measured angular size at 8.46 GHz of the radio afterglow is ~ 75 mas around seven to ten days after the flare and has no noticeable variation in diameter during this period (Gaensler et al. 2005; Cameron et al. 2005). At a distance of $d = 15.1$ kpc, this angular size implies a subluminal speed of $\sim 0.35c$ for the averaged projected expansion and an apparent radius of $R_{\perp} = 9 \times 10^{15}$ cm. So, if the outflow is spherical at this time (i.e. $R = R_{\perp}$), we obtain the constraint on the outflow energy, i.e. $E \simeq 10^{44} n_0$ ergs¹. If, instead, the outflow is mildly beamed in the non-relativistic phase, then the half opening angle θ satisfies $\sin\theta = R_{\perp}/R = 0.4(E_{46}/n_0)^{-1/5}$. In any case, the real kinetic energy (after beaming correction) of the outflow is about $10^{44} - 10^{45}$ ergs for a typical ISM with $n = 1$ cm⁻³ and $d = 15.1$ kpc. It is more reasonable to believe that the outflow becomes approximately spherical at the non-relativistic phase when the sideways expansion takes place (Livio & Waxman 2000). In the following we will focus on the spherical outflow case with $E = 10^{44} n_0$ ergs. The apparent radius should increase with time as $R \propto t^{2/5}$ in the non-relativistic phase, so it will increase by a factor of 1.15 from 7 to 10 days. This is consistent with the fact that there is no noticeable observed variation of the angular size during the period².

2.2. The light curves of the radio afterglow

As the blast wave sweeps up the surrounding medium, the shock accelerates electrons and amplifies the magnetic field in the swept-up matter (Blandford & Eichler 1987). The afterglow emission arises from synchrotron radiation of these shocked electrons in the magnetic field. The electron energy distribution in the downstream of the shock usually manifests as a single power law or broken power law. The radio-band spectra show a gradual steepening with time, with a single power-law index of $\beta_1 = 0.62 \pm 0.02$ around $t = 7$ d, while at $t = 23$ d, $\beta_2 = -0.91 \pm 0.08$ (Cameron et al. 2005). There are also reports that a possible break exists in the radio-band spectrum at early epoches (Gaensler et al. 2005). For example, at about 9 days after the giant flare, the measured power law spectral index between 4.8 and 8.6 GHz is ~ -1.0 , while between 2.4 and 4.8 GHz the index is ~ -0.66 (Gaensler et al. 2005). The steepening of the light curve decay with frequency also favors that there is a spectral break between

240 MHz and 8.46 GHz in the synchrotron blast wave model. This break is unlikely to be the cooling break because the cooling frequency is much higher than the radio band (see Eq.2). As suggested by Li & Chevalier (2001) to explain the afterglows of GRB991208 and GRB000301C, we consider that this break is caused by an intrinsic break in the energy distribution of the shock-accelerated electrons, which takes the form of

$$\frac{dN_e}{d\gamma_e} = \begin{cases} C\gamma_e^{-p_1}, & \text{if } \gamma_{\min} < \gamma_e < \gamma_b \\ C\gamma_b^{p_2-p_1}\gamma_e^{-p_2}, & \text{if } \gamma_e > \gamma_b \end{cases} \quad (1)$$

where γ_{\min} and γ_b are the minimum and break Lorentz factors respectively. The observed synchrotron spectrum of the Crab Nebula supports the intrinsic break in the injected particle spectrum (Amato et al. 2000). Similarly, we assume that the ratio of the break energy and the minimum energy, $R_b \equiv \gamma_b/\gamma_{\min}$, remains essentially a constant in time so that the relative shape of the distribution is time invariant (Li & Chevalier 2001). From the values of β_1 and β_2 , we infer $p_1 \simeq 2.2$ and $p_2 \simeq 3.0$.

Assuming that shocked electrons and the magnetic field acquire constant fractions (ϵ_e and ϵ_B) of the total shock energy density, we get $\gamma_{\min} \simeq \epsilon_e \frac{p_1-2}{p_1-1} \frac{m_p}{m_e} (\Gamma - 1)$ and $B = (16\pi\epsilon_B\beta^2 nm_p c^2)^{1/2} = 1.4 \times 10^{-2} \epsilon_{B,-1}^{1/2} E_{44}^{1/5} t_1^{-3/5} n_0^{3/10}$ G. Thus we can obtain the break frequency corresponding to γ_{\min} , the break frequency corresponding to the electron break caused by the synchrotron cooling, and the peak flux of the spectrum, which are given by

$$\begin{aligned} \nu_m &= 3 \times 10^5 \left[\frac{3(p_1-2)}{p_1-1} \right]^2 \left(\frac{\epsilon_e}{0.3} \right)^2 E_{44} t_1^{-3} n_0^{-1/2} \epsilon_{B,-1}^{1/2} \text{Hz} \\ \nu_c &= 1.4 \times 10^{18} \epsilon_{B,-1}^{-3/2} E_{44}^{-3/5} n_0^{-9/10} t_1^{-1/5} \text{Hz} \\ F_{\nu_m} &= 95 E_{44}^{4/5} t_1^{3/5} n_0^{7/10} \epsilon_{B,-1}^{1/2} (d/15.1 \text{ kpc})^{-2} \text{Jy}. \end{aligned} \quad (2)$$

For a broken power-law electron distribution described by Eq.(1), the light curves at the frequencies below and above the break frequency ν_b (which is the synchrotron frequency corresponding to γ_b) are different. According to the afterglow theory, the light curves in the non-relativistic phase should have the decay slopes of $(21 - 15p_1)/10$ and $(21 - 15p_2)/10$, respectively. For $p_1 = 2.2$ and $p_2 = 3$, the predicted slopes are in agreement with the observed ones (i.e. $\alpha_1 = -1.43 \pm 0.17$ for 240 MHz and $\alpha_2 = -2.63 \pm 0.13$ for 8.46 GHz) of the radio afterglow data (Cameron et al. 2005), if the break frequency ν_b locates between 240 MHz and 8.46 GHz. The 4.86 GHz light curve shows a break around $t = 9$ d, which implies that, in the above picture, ν_b just crosses 4.86 GHz at this time. This then suggests $R_b = 130(\epsilon_e/0.3)^{-1} \epsilon_{B,-1}^{-1/4} E_{44}^{-1/2} n_0^{1/4}$. The shifting of ν_b to lower frequencies would make 1.43 GHz light curve decay faster at late times.

The flux density at 1.43 GHz is

$$F_{\nu} = 0.26 E_{44}^{\frac{5p_1+3}{10}} n_0^{\frac{19-5p_1}{20}} \epsilon_{B,-1}^{\frac{p_1+1}{4}} \left(\frac{\epsilon_e}{0.3} \right)^{p_1-1} t_1^{\frac{21-15p_1}{10}} \left(\frac{d}{15.1 \text{ kpc}} \right)^{-2} \text{Jy}, \quad (3)$$

¹The discrepancy between the isotropic gamma-ray energy and the kinetic energy of the afterglow may be naturally expected within the magnetar framework as the prompt hard spike emission taps the magnetic energy, while the afterglow is only related to the kinetic energy (Zhang & Kobayashi 2005). On the other hand, this discrepancy could be alleviated by a denser environment.

²After the submission of the paper, more observation data of the angular size at time from 10 to 20 days are reported in Gaensler et al. (2005). The angular size shows a slow increase with time, being consistent with the $R \propto t^{2/5}$ relation.

where the coefficient is calculated for $p_1 = 2.2$. At $t = 9.87d$, the observed flux density at 1.43 GHz is $96 \pm 2\text{mJy}$ (Cameron et al. 2005). So, for typical parameter values of $E = 10^{44}\text{ergs}$, $n = 1\text{cm}^{-3}$, $d = 15.1\text{kpc}$ and $\epsilon_e = 0.3$, we infer $\epsilon_B = 0.04$. This equipartition factor is close to that inferred for GRB afterglows (e.g. Wijers & Galama 1999; Panaitescu & Kumar 2001) and corresponds to a magnetic field of $\sim 10\text{mG}$ in the shocked medium. Nevertheless, we should note that the observations are all in the power-law domain and the spectral transitions (e.g. ν_m and ν_c) have not been observed, which makes the physical parameters of this flare not well constrained.

We have also carried out detailed numerical calculations of the radio afterglow light curves at five frequencies, i.e. 8.46 GHz, 4.86 GHz, 1.43 GHz, 608 MHz and 240 MHz. The numerical model contains more careful treatments to the blast wave dynamics during the trans-relativistic stage (Huang et al. 2000) and the broken power-law electron distribution³. It is found that the numerical model can give a satisfactory fit to the light curve data over five radio frequencies, as shown in Fig.1. The theoretic light curve of 610MHz are somewhat above the observation data. This discrepancy is also evident in the power-law fit of the radio spectra in Fig.1 of Cameron et al. (2005). The parameter values used in the fit are consistent with those constrained by the above analytic study⁴. An interesting finding is that, unlike GRB radio afterglows that usually peak around a week after the burst, the predicted SGR radio afterglows are significantly stronger at earlier times. This calls for an even more rapid follow-up in the radio band.

3. OPTICAL, INFRARED AND X-RAY AFTERGLOWS OF GIANT FLARES AND INTERMEDIATE BURSTS OF SGRs

SGR afterglows have been detected only in the radio band so far. Within the above picture, it is natural to expect optical and infrared afterglows as well produced by the same relativistic fireball accompanying the SGR giant flares. At the early time $t < t_{\text{nr}}$, the blast wave is relativistic and its emission spectrum is characterized by

$$\begin{aligned}\nu_m &= 7.5 \times 10^{10} \left[\frac{3(p-2)}{p-1} \right]^2 \left(\frac{\epsilon_e}{0.3} \right)^2 E_{44}^{1/2} \epsilon_{B,-1}^{1/2} t_{-1}^{-3/2} \text{Hz} \\ \nu_c &= 1.1 \times 10^{18} \epsilon_{B,-1}^{-3/2} E_{44}^{-1/2} n_0^{-1} t_{-1}^{-1/2} \text{Hz} \\ F_{\nu_m} &= 15 \epsilon_{B,-1}^{1/2} E_{44} n_0^{1/2} (d/15.1\text{kpc})^{-2} \text{Jy}.\end{aligned}\quad (4)$$

The optical flux density at R -band ($4.55 \times 10^{14}\text{Hz}$) is

$$F_R = 30 \left(\frac{\epsilon_e}{0.3} \right)^{p-1} \epsilon_{B,-1}^{\frac{p+1}{4}} E_{44}^{\frac{p+3}{4}} n_0^{1/2} t_{-1}^{-\frac{3(p-1)}{4}} \left(\frac{d}{15.1\text{kpc}} \right)^{-2} \text{mJy}, \quad (5)$$

where $p \simeq 2.4$ is the power-law index of the electron distribution inferred from the global spectrum $F_\nu \propto \nu^{-0.68 \pm 0.02}$ (Cameron et al. 2005). For typical parameter values and the inferred value $\epsilon_B = 0.04$ from the radio afterglows, the magnitude of the optical afterglow at $t = 0.1d$ is about $m_R \simeq 13$. Considering that, for an initial beamed outflow, the isotropic equivalent energy in the relativistic phase may be larger than that in the non-relativistic

spherical phase, the above estimate is conservative. Because the characteristic synchrotron frequency ν_m at early times is generally below the optical frequency for an initial Lorentz factor of $\Gamma_0 \sim 10$, the optical afterglow reaches its peak at the deceleration time of the relativistic outflow, which is $t_{\text{dec}} = 90 E_{44}^{1/3} n_0^{-1/3} \Gamma_{0,1}^{-8/3} \text{s}$. At this time, $\nu_m = 1.1 \times 10^{14} (\epsilon_e/0.3)^2 \epsilon_{B,-1}^{1/2} n_0^{1/2} \Gamma_{0,1}^4 \text{Hz}$, and the optical afterglow has a flux density of

$$F_R = 5 \left(\frac{\epsilon_e}{0.3} \right)^{p-1} E_{44} \epsilon_{B,-1}^{\frac{p+1}{4}} n_0^{\frac{p+1}{4}} \Gamma_{0,1}^{2(p-1)} \left(\frac{d}{15.1\text{kpc}} \right)^{-2} \text{Jy}.\quad (6)$$

Such a bright optical afterglow would be easily detected by rapid response detectors, such as Ultraviolet/Optical Telescope (UVOT) on *Swift* and Robotic Optical Transient Search Experiment (ROTSE), if the optical extinction to the source is not very large. However, SGR 1806-20 has a low Galactic latitude and has optical extinction of $A_V \sim 30\text{mag}$ (Eikenberry et al. 2001). This makes it impossible to observe the optical afterglow from this SGR. The difficulty also applies for the other two SGRs at low Galactic latitudes, SGR 1900+14 and SGR 1627-41, whose extinction is also large (Vrba et al. 2000; Wachter et al. 2004). The R -band extinction of SGR 1900+14 is moderate, i.e. $A_R \sim 7\text{mag}$ (Akerlof et al. 2000), leaving some hope for optical afterglow detection at its peak. The best target for optical follow-up observations among the four known SGRs is SGR 0526-66, which lies in the Large Magellanic Cloud and has $A_V \simeq 1$. At a distance of $d \simeq 50\text{kpc}$, the optical afterglow of a similar giant flare from this SGR is expected to be bright enough for follow-ups. Even the less rare intermediate bursts with the isotropic energies ranging from 10^{41} to 10^{43} ergs (e.g. Golenetskii et al. 1984; Guidorzi et al. 2004) are expected to have optical afterglows brighter than $m_R \simeq 23$ at $t < 0.1d$ for SGR 0526-66. This is well above the *Swift* UVOT sensitivity. Detecting such an optical afterglow would further test the blast wave model and provide more detailed information of the early evolution of a fireball.

Because of the high optical extinction of low-latitude SGRs, infrared observations to giant flares and intermediate bursts appear very useful. The K band flux density would be, according to Eq. (6), $F_{2.2\mu\text{m}} \sim 3\text{mJy}$ or $m_K \simeq 13$ at $t = 1d$ for typical parameter values to model the radio afterglow of the December 27 giant flare. Such a bright infrared afterglow could be well detected by ground-based infrared telescopes. An example of the (unabsorbed) light curves of the infrared and optical afterglows calculated with the numerical model for the radio afterglows is also shown in Fig.2. The flux of the X-ray afterglow can be estimated in the same way. For the above typical parameter values, we find the flux at $t = 0.1d$ is about $F_X \simeq 2.6 \times 10^{-10} \text{ergcm}^{-2}\text{s}^{-1}$. This flux is, however, much dimmer than the observed X-ray flux of the SGR 1900+14 giant flare (Woods et al. 2001), which is thought to be originated from the neutron star surface immediately after the burst.

³The code also takes account of the re-derived electron distribution by Huang & Cheng (2003) for afterglows in the deep Newtonian phase.

⁴For a smaller source distance d (Cameron et al. 2005), E/n should be correspondingly smaller in order to be consistent with the measured angular size. As a result, a larger value for ϵ_B is then inferred. However, the global agreement of the radio afterglow behavior with the blast wave model remains unchanged.

4. DISCUSSIONS

We have shown that the radio afterglow behavior of the December 27 giant flare of SGR 1806-20, including the angular size and multi-frequency light curves, provides a first piece of clear evidence that the fireball/blast wave model indeed works in SGRs as well. The polarization emission detected in the radio afterglow (Gaensler et al. 2005; Cameron et al. 2005) at a comparable level (1% – 3%) to GRB afterglows (Covino et al. 1999; Wijers et al. 1999) is also consistent with the blast wave model. The initial Lorentz factor of the outflow that drives the blast wave is not well constrained, because only the late-time radio afterglow is available up to now. The composite of the

relativistic outflow is also unknown and could be normal baryon matter as well as relativistic electron-positron dominated wind since both could drive relativistic blast waves when they are interacting with the surrounding medium.

XYW would like to thank Y. F. Huang, D. M. Wei, Z. Li and T. Lu for useful discussions. We also thank S. Kulkarni and B. Gaensler for informative communications. This work was supported by the Special Funds for Major State Basic Research Projects, the National 973 Project (NKBRF G19990754), the National Natural Science Foundation of China under grants 10403002, 10233010 and 10221001. B. Zhang is supported by NASA NNG04GD51G and a NASA Swift GI (Cycle 1) program.

REFERENCES

- Akerlof, C. et al. 2000, ApJ, 542, 251
 Amato, E., et al., 2000, A&A 359, 1107
 Blandford, R. & Eichler, D. 1987, *Phys. Rep.* 154, 1
 Boggs, S. et al. 2005, GCN Circ. 2936
 Borkowski, J. et al. 2004, GCN Circ. 2920
 Cameron, P. B., et al. 2005, Nature, submitted, astro-ph/0502428
 Cheng, K. S. & Wang, X. Y., 2003, ApJ, 593, L85
 Corbel, S. & Eikenberry, S. S. 2004, A&A, 419, 191
 Covino, S. et al. 1999, A&A, 348, L1
 Eikenberry, S. S. et al. 2001, ApJ, 563, L133
 Frail, D., Kulkarni, S. R., & Bloom, J., 1999, Nature, 398, 127
 Gaensler, B. M., et al. 2005, Nature, in press, astro-ph/0502393
 Golenetskii, S. V., Ilyinskii, V. N. & Mazets, E. P. 1984, Nature, 307, 41
 Guidorzi, C. et al. 2004, A&A, 416, 297
 Huang, Y. F., Dai, Z. G. & Lu, T., 1998, Chinese Phys. Lett., 15, 775
 Huang, Y. F., Gou, L. J., Dai, Z. G., & Lu, T. 2000, ApJ, 543, 90
 Huang, Y. F., Cheng, K. S. 2003, MNRAS, 341, 263
 Hurley, K., et al. 1999, Nature, 397, 41
 Hurley, K. et al. 2004, GCN Circ. 2921
 Li, Z.-Y. & Chevalier, R.A., 2001, ApJ, 551, 940
 Livio, M. & Waxman, E. 2000, ApJ, 538, 187
 Mazets, E. P., et al. 1979, Nature, 282, 587
 Mazets, E. P. et al. 2004, GCN Circ. 2922
 Mészáros, P. & Rees, M. J., 1997, ApJ 476, 232
 Palmer, D. et al. 2004, GCN Circ. 2925
 Panaitescu, A., Kumar, P., 2001, ApJ, 560, L49
 Smith, E. et al., 2005, GCN Circ. 2927
 Thompson, C. & Duncan, R. C., 1995, MNRAS, 275, 255
 Thompson, C. & Duncan, R. C., 2001, ApJ, 561, 980
 Vrba, F. J. et al. 2000, ApJ, 533, L17
 Wachter et al., 2004, ApJ, 615, 887
 Wijers, R. A. M. J., & Galama, T. J., 1999, ApJ, 523, 177
 Wijers, R. A. M. J., et al. 1999, ApJ, 523, L33
 Woods, P. M. et al., 2001, ApJ, 552, 748
 Zhang, B. & Kabayashi, S., 2005, ApJ, in press, astro-ph/0404140

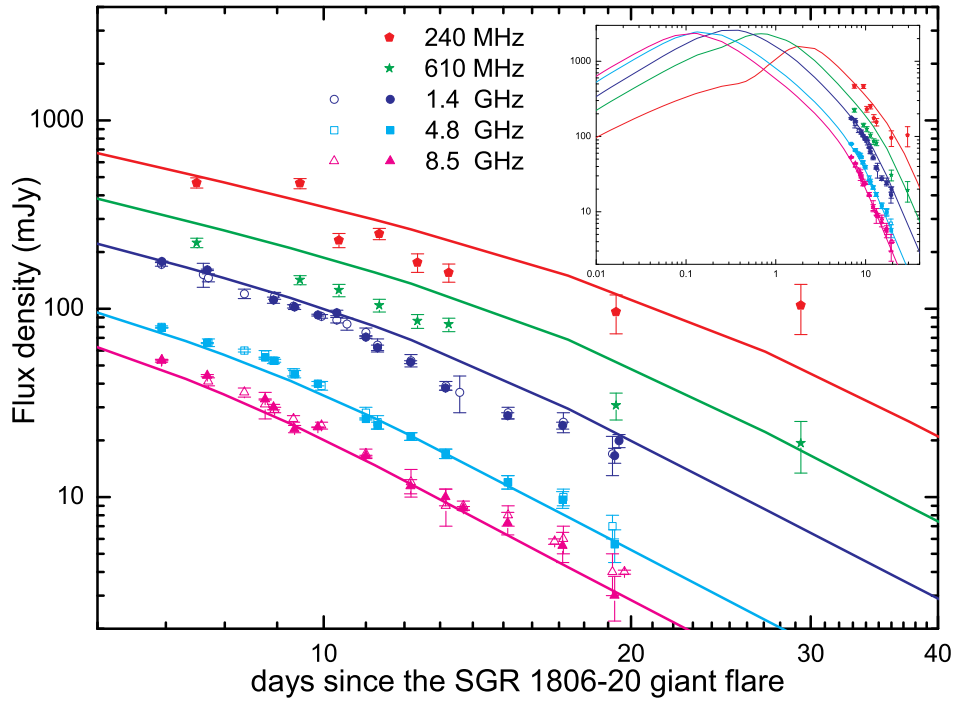


FIG. 1.— Numerical fits of the radio afterglows of the December 27 giant flare from SGR 1806-20 with the blast wave model. The data are taken from Gaensler et al. (2005) (open symbols) and Cameron et al. (2005) (solid symbols). The parameter values used in the fits are $E = 10^{44}$ erg, $n = 1\text{cm}^{-3}$, $\Gamma_0 = 10$, $\epsilon_e = 0.32$, $\epsilon_B = 0.1$, $p_1 = 2.2$, $p_2 = 3.2$, $R_b = 150$ and $d = 15.1\text{kpc}$. The inset shows these light curves over a longer time range.

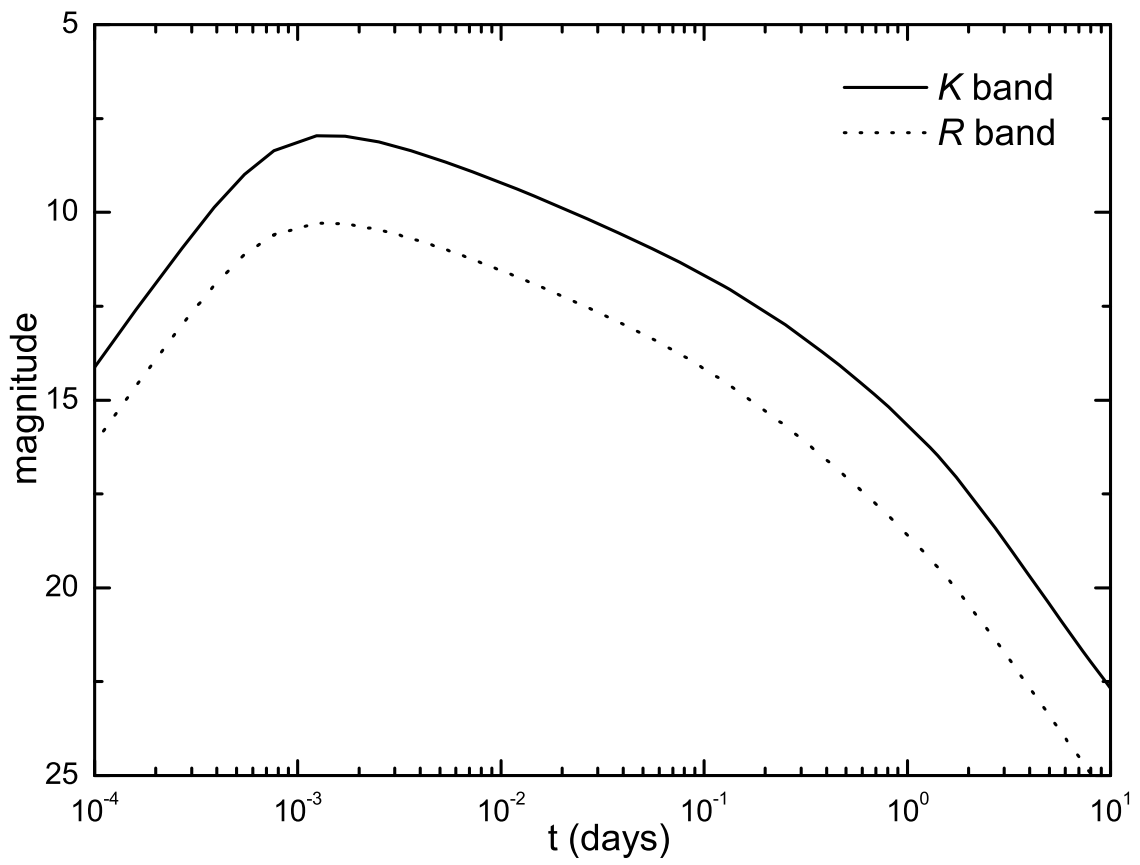


FIG. 2.— The predicted optical (R -band) and infrared (K -band) afterglows of a giant flare similar to the December 27 event. Parameter values used are the same as those in the fits of Fig. 1.